Many-Body Localization in Dipolar Systems

Citation

Published Version

Permanent link

Terms of Use

Share Your Story

Many-Body Localization in Dipolar Systems

N. Y. Yao,[1] C. R. Laumann,[1,2,3,4] S. Gopalakrishnan,[1] M. Knap,[1,4] M. Müller,[5] E. A. Demler,[1] and M. D. Lukin[1]

[1]*Department of Physics, Harvard University, Cambridge, Massachusetts 02138, USA*
[2]*Perimeter Institute for Theoretical Physics, Waterloo, Ontario N2L 2Y5, Canada*
[3]*Department of Physics, University of Washington, Seattle, Washington 98195, USA*
[4]*ITAMP, Harvard-Smithsonian Center for Astrophysics, Cambridge, Massachusetts 02138, USA*
[5]*The Abdus Salam International Center for Theoretical Physics, Strada Costiera 11, 34151 Trieste, Italy*

Systems of strongly interacting dipoles offer an attractive platform to study many-body localized phases, owing to their long coherence times and strong interactions. We explore conditions under which such localized phases persist in the presence of power-law interactions and supplement our analytic treatment with numerical evidence of localized states in one dimension. We propose and analyze several experimental systems that can be used to observe and probe such states, including ultracold polar molecules and solid-state magnetic spin impurities.

Introduction.—Statistical mechanics is the framework that connects thermodynamics to the microscopic world. It hinges on the assumption of equilibration; when equilibration fails, so does much of our understanding. In isolated quantum systems, this breakdown is captured by the phenomenon known as many-body localization (MBL) [1–29]. Many-body localized phases conduct neither matter, charge, nor heat. Moreover, they can exhibit symmetry breaking and topological order in dimensions normally forbidden by Mermin-Wagner-type arguments [20,26]. To date, none of these phenomena has been observed in experiments, in part because of the isolation required to avoid thermalization.

In this Letter, we investigate dilute dipolar systems as a platform for realizing MBL phases and studying the associated localization phase transition. Our work is motivated by recent experimental advances that make it possible to produce and probe isolated, strongly interacting ensembles of disordered particles, as found in systems ranging from trapped ions [30] and Rydberg atoms [31,32] to ultracold polar molecules [33,34] and spin defects in solid-state systems [35–38]. The presence of strong interactions in these systems underlies their potential for exploring physics beyond that of single-particle Anderson localization [1]. However, the power-law decay of those interactions immediately raises the following question: Can localization persist in the presence of such long-range interactions? Indeed, Anderson observed in his seminal paper that long-ranged *hopping*, $t \sim 1/r^{\alpha}$, delocalizes any putatively localized single-particle states for $\alpha \leq d$, with d the dimension of space. In what follows, we consider the generalization of Anderson's criterion to the *interacting* power-law regime and produce a necessary condition for localization with such interactions [6–9]. To support these considerations, we carry out an extensive numerical analysis of power-law interacting systems in $d = 1$ spatial dimensions. With this criterion in hand, we analyze the feasibility of observing MBL states in two complementary ultracold polar molecule proposals, wherein the power
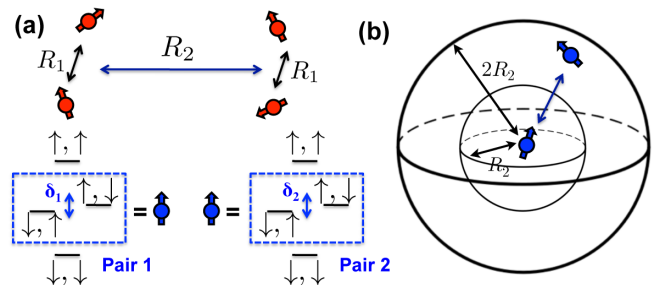

FIG. 1 (color online). (a) Schematic of four-spin resonance structure. Each pair of (red) spins at separation R_1 forms a pseudospin (blue) with the level structure shown below. (b) A pseudospin at the origin resonates with another pseudospin in a shell $R_2 < r < 2R_2$.

laws, interaction scales, and dimensionality may be tuned. Finally, we generalize our analysis to solid-state systems where localization can be studied in the quantum dynamics of magnetic spin impurities.

Conditions for localization.—In localized systems, injections of energy propagate at most a finite distance even after infinite time. This is obviously inconsistent with the proliferation of long-range resonances through which energy may be transported. In the following, we identify resonant degrees of freedom and ask whether the number of such resonances diverges at large scales; such divergence suggests the existence of a percolating network that conducts energy [6–9]. We consider a general two-body Hamiltonian of spin 1/2 particles with conserved total S^z,

$$H = \sum_i \epsilon_i S_i^z - \sum_{ij} \frac{t_{ij}}{|r_{ij}|^{\alpha}}(S_i^+ S_j^- + \text{H.c.}) + \sum_{ij} \frac{V_{ij}}{|r_{ij}|^{\beta}} S_i^z S_j^z, \quad (1)$$

where ϵ_i is a site-dependent disorder field of bandwidth W, while α and β are the exponents governing the power-law decay of spin flip-flops and spin interactions, respectively [39]; we assume $\beta \leq \alpha$, consistent with all physical

TABLE I.　Critical dimensions for MBL with power laws.

	Unmixed $\alpha = \beta$ [8,9]	Anisotropic $\beta < \alpha$	Multipole $\beta < \alpha$
Hopping	$d < \alpha$	$d < \alpha$	$d < \alpha$
Small pairs	$d < \beta$	$d < \beta$	$d < \beta + 2$
Extended pairs	$d < \beta/2$	$d < \alpha\beta/(\alpha + \beta)$	$d < \alpha(\beta + 2)/(\alpha + \beta + 4)$
Iterated pairs	$d < \beta/2$	$d < \beta/2$	$d < (\beta + 2)/2$

realizations of which we are aware. Clearly, the analysis applies to general long-range interacting two-level systems with a conserved charge.

We identify resonant pairs of spins as those for which $|\epsilon_i - \epsilon_j| \lesssim t_{ij}/|r_{ij}|^\alpha$; the expected number of resonant spins at a distance $R_1 < |r_{ij}| < 2R_1$ from a central spin is

$$N_1(R_1) \sim (\rho R_1^d) \frac{t/R_1^\alpha}{W}, \qquad (2)$$

where ρ is the density of spins. If $N_1(R_1)$ diverges as $R_1 \to \infty$, that is, if $d > \alpha$, then any spin resonates with arbitrarily distant spins and localization is impossible; this is precisely Anderson's criterion for single-particle localization. In the critical case, $d = \alpha$, a detailed renormalization group treatment confirms subdiffusive but delocalized behavior for the noninteracting case [1,40,41].

As shown in Fig. 1(a), the two strongly hybridized central levels of a resonant pair define a new pseudospin degree of freedom (blue arrows) with local splittings $\delta \sim t/R_1^\alpha$. Pseudospins can exchange energy through the interaction V since the operators S^z have spin-flip matrix elements between the two pseudospin states [6–9]. Two pseudospins separated by R_2 resonate if $\delta_1, \delta_2 > V(R_2) \gtrsim |\delta_1 - \delta_2|$ [42]. The number of such resonances available in a shell from distance R_2 to $2R_2$ around a fixed pseudospin [Fig. 1(b)] is

$$N_2(R_1, R_2) \sim [n_1(R_1)R_2^d] \frac{V/R_2^\beta}{t/R_1^\alpha}, \qquad (3)$$

where $n_1 = \rho N_1$ is the density of pseudospins. As before, if N_2 diverges as $R_2 \to \infty$, large-scale pseudospin resonances induce delocalization [6–9]. There are two limits. The simplest case occurs when one holds the pair size R_1 fixed as R_2 diverges; this "small pairs" condition yields a localization criterion $d < \beta$. The second case requires optimizing R_1 as R_2 grows in order to saturate the probability of pseudospin resonance. More precisely, one should replace $(V/R_2^\beta)/(t/R_1^\alpha) \to \min[1, (V/R_2^\beta)/(t/R_1^\alpha)]$ in Eq. (3). The optimum arises for $R_1 \sim R_2^{\beta/\alpha}$, yielding a more stringent "extended pairs" condition, $d < \alpha\beta/(\alpha + \beta)$.

It is clear that one can continue iterating the construction of pair resonances. However, the resulting criteria for MBL saturate after the third level [42,43],

$$N_3(R_1, R_2, R_3) \sim [n_2(R_1, R_2)R_3^d] \frac{V/R_3^\beta}{V/R_2^\beta}, \qquad (4)$$

where $n_2 = n_1 N_2$ is the density of pseudo-pseudospins. There are three limits as R_3 diverges. Holding R_1, R_2 fixed reproduces the small-pairs criterion. Holding R_1 fixed but optimizing $R_2 \sim R_3$ [to saturate the probability of

resonance in Eq. (4)] yields a new, "iterated pairs" criterion $d < \beta/2$. Finally, optimizing both $R_1 \sim R_2^{\beta/\alpha}$ and $R_2 \sim R_3$ reproduces the extended pairs criterion.

The above results hold for generic anisotropic distributions of t_{ij}, V_{ij} (first two columns of Table I). In certain cases, which we term "multipole," the effective matrix elements that arise in the four-spin construction cancel at leading order. To be precise, this cancellation occurs when the derivatives of the interaction scale as the interaction divided by the distance separating the spins. This can be understood within a multipole expansion (for $R_1 < R_2$), which amounts to replacing $V/R_2^\beta \to V R_1^2/R_2^{\beta+2}$ for N_2 and analogously for subsequent iterations (last column of Table I).

A few comments are in order. (1) In the anisotropic and unmixed ($\alpha = \beta$) cases, the iterated pairs criterion $d < \beta/2$ is always most stringent, a result first derived in Refs. [8,9]. (2) In the multipole case, for $\alpha < \beta + 4$, the extended-pairs criterion is most stringent, while for $\alpha > \beta + 4$, the iterated-pairs criterion dominates. (3) The case of an Anderson insulator with Coulomb interactions corresponds to the $\alpha \to \infty$ limit of the multipole case, giving an upper critical dimension of $d_c = 1.5$. (4) The case of interacting dipoles with $\alpha = \beta = 3$ also gives $d_c = 1.5$. Interestingly, the orientation dependence of the dipolar interaction is sufficiently isotopic to enable a multipole expansion. Thus, in experiments that can realize $\alpha = 6$, $\beta = 3$ (as will be discussed later), $d_c \approx 2.3$ [42].

Ultimately, all of the resonance arguments described above rely upon the analysis of finite subsets of spins. While providing useful insights, such arguments must be viewed as heuristic. To supplement, we have performed extensive exact diagonalization studies of Eq. (1) in $d = 1$ for $\alpha = \beta = 1, 3/2, 2, 3$. We consider periodic systems up to size $L = 14$ at the filling fraction $\nu = 1/2$. The random fields are drawn from a uniform distribution of width W, the interaction $V_{ij} = V = 2$, and the hopping $t_{ij} = t = 1$. The presence of a many-body localized phase may be detected by the finite-size flow of the dynamic polarization D, a measure of spin transport across the 1D system at infinite temperature [11]. We perturb each eigenstate with a small (long-wavelength) inhomogeneous spin modulation of the form $\hat{F} = \sum_j S_j^z e^{i2\pi j/L}$ and measure the relaxation of this inhomogeneous polarization at infinite time. For each disorder realization η and eigenstate k, the dynamic polarization is given by

$$D_\eta^k = 1 - \frac{\langle k|\hat{F}^\dagger|k\rangle\langle k|\hat{F}|k\rangle}{\langle k|\hat{F}^\dagger\hat{F}|k\rangle}. \qquad (5)$$

We then define D as the infinite temperature disorder average of D_η^k. As $L \to \infty$, in the ergodic phase, one expects $D \to 1$
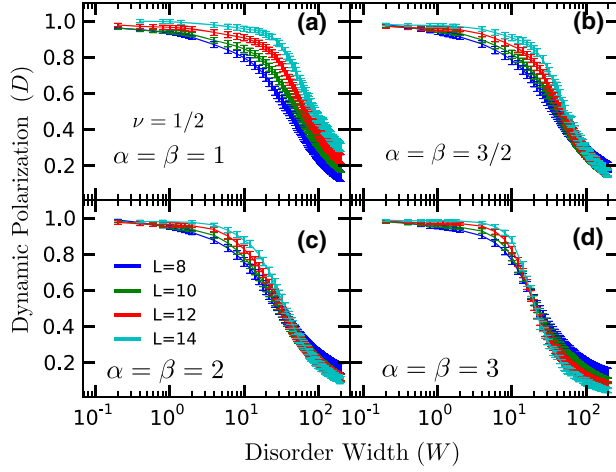
FIG. 2 (color online). Finite-size scaling of the long-time dynamic polarization for Eq. (1) in $d = 1$ (with units $t = 1$, $V = 2$) with (a) $\alpha = \beta = 1$, (b) $\alpha = \beta = 3/2$, (c) $\alpha = \beta = 2$, and (d) $\alpha = \beta = 3$. The lack of flow reversal in (a) suggests delocalization at all disorders. The sharpening of the crossover as a function of increasing system size in (d) suggests the existence of a phase transition at approximately $W_c \approx 10$ into an MBL phase. The flow at intermediate power laws (b) is inconclusive.

FIG. 3 (color online). (a) Schematic of the one-dimensional tube geometry with strong confinement in the $\hat{y}$ and $\hat{z}$ directions and hopping in the $\hat{x}$ direction. (b) Dipolar molecules in each 1D tube are subject to an optical speckle pattern that generates an effective random on-site chemical potential for the hopping molecules. (c) Schematic of the dipolar "spin" hopping model. Molecules pinned with dilution in the deep optical lattice may exchange rotational excitations. (d) Effective rotational level structure of a polar molecule, with $|\uparrow\rangle = |1, 1\rangle$, $|\downarrow\rangle = |0, 0\rangle$ shown for the $\alpha = \beta = 3$ rotor model. (e) Level structure of two polar molecules for the $\alpha = 6$ rotor model, wherein hopping is mediated by a second-order dipolar process.

since the initial inhomogeneity relaxes away; in the MBL phase, one expects $D \to 0$ since there is no transport.

The results are shown in Fig. 2. For all exponents, we find that the finite-size flow of D is consistent with delocalization at weak disorder. At strong disorder, for $\alpha = 2, 3$, there are signs of flow reversal, consistent with a transition into a MBL phase, while for $\alpha = 1$, the flow remains toward delocalization for all disorder strengths. Owing to the small sizes accessible to exact diagonalization, flow reversal does not prove the existence of a transition; however, for $\alpha = 3$, the combination of relatively clear flow and the previous theoretical argument suggests the existence of a MBL phase. The strong disorder flow at intermediate exponents $\alpha = 3/2$ is inconclusive. Accordingly, for $d = 1$, we numerically bound the critical power law with $1 < \alpha_c < 3$, noting that the extended-pairs criterion gives $\alpha_c = 2$. The difficulty of investigating a MBL transition in small-size numerics emphasizes the importance of controlled experiments.

Experimental realizations.—Next, we analyze two classes of experimentally accessible systems in which MBL phases may be realized. First, we consider an array of polar molecules confined to a one-dimensional tube geometry (via an optical lattice) as depicted in Figs. 3(a) and 3(b) [33]. The optical lattice is strongly confining along the $\hat{y}$ and $\hat{z}$ axes, but molecules can tunnel with nearest-neighbor hopping strength t along the tube in the $\hat{x}$ direction ($\alpha \to \infty$). The molecules are prepared in their rovibrational ground state and are subject to a static electric field E perpendicular to the tube direction. The applied electric field weakly aligns the molecules along the field direction, inducing a finite dipole moment d and a long-range electric dipole-dipole interaction between the molecules $V \sim d^2/R^3$ ($\beta = 3$). By ensuring that the dipolar
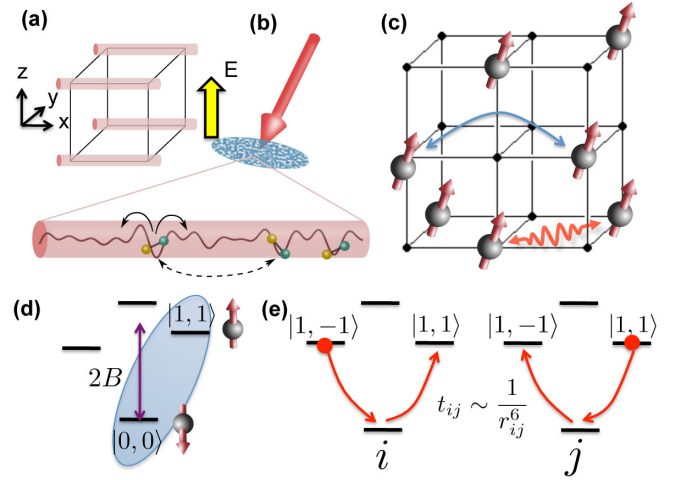
interaction strength is much weaker than the rotational splitting B [Fig. 3(d)], all molecules remain in the rovibrational ground state. Finally, an optical speckle field may be superimposed on top of the underlying lattice, introducing on-site potential disorder with strength W controlled by the laser intensity [Fig. 3(b)] [44].

The magnitude of the electric field tunes the strength of the dipolar interaction $V \sim d^2$. In the limit $E \to 0$, the interaction strength $V \to 0$, and the resulting nearest-neighbor Hamiltonian can be fermionized. This noninteracting model is completely Anderson localized in the presence of any disorder. With the addition of local interactions, the existence of a MBL phase has been established both theoretically and numerically [4,5,10–12]. According to the criterion in Table I, the MBL phase ought to also survive the introduction of long-range dipolar interactions. To confirm this expectation and further establish an experimentally relevant phase diagram, we perform exact diagonalization for molecular filling fractions $\nu = 1/2, 1/3, 1/4$ up to system sizes of $L = 16, 18, 20$, respectively [Fig. 4(a)]. As depicted in Fig. 4(b), we obtain the MBL phase diagram as a function of interaction strength, filling fraction, and speckle intensity [44].

Next, we consider disordered arrays of interacting molecules with a fixed center-of-mass position and focus on the dynamics of rotational excitations [Fig. 3(c)]. In the deep lattice limit, the orbital motion of the molecules is pinned, and the residual rotational degree of freedom is governed by an effective Hamiltonian, $H_m = BJ^2 - d^z E$ [45]. A combination of electric and magnetic fields allows us to
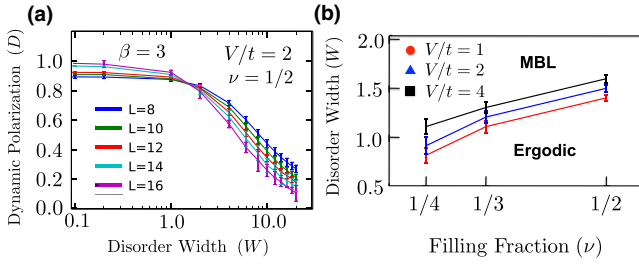
FIG. 4 (color online). Exact diagonalization study of Eq. (1) with nearest-neighbor hopping ($\alpha \to \infty$) and dipolar interactions ($\beta = 3$). Random fields are drawn from a uniform distribution of width W. (a) Finite-size scaling of the long-time dynamic polarization. The finite-size flow suggests a delocalization phase transition at $W_c \approx 1.4t$. (b) MBL phase boundaries determined by finite-size flow for $V/t = 1, 2, 4$.

isolate an effective two-level system: $|\downarrow\rangle = |J = 0, m_j = 0\rangle$ and $|\uparrow\rangle = |J = 1, m_j = 1\rangle$ [Fig. 3(d)] [46]. The rotors interact via electric dipole-dipole interactions with the Hamiltonian, $H_{dd} = \frac{1}{2}\sum_{i\neq j}(\mathbf{d_i}(1 - 3\hat{r}_{ij}\hat{r}_{ij})\mathbf{d_j}/r_{ij}^3)$, where $\mathbf{d}$ is the dipole moment operator. Projecting H_{dd} onto the two-level subspace $\{|\downarrow\rangle, |\uparrow\rangle\}$ and keeping only secular terms yields the Hamiltonian of Eq. (1) with effective on-site fields given by $\epsilon_i = \sum_{j\neq i}d_s d_a/r_{ij}^3$, $\alpha = \beta = 3$, and $d_{s,a} = 1/2(\langle 1|d^z|1\rangle \pm \langle 0|d^z|0\rangle)$. Assuming Poissonian (uncorrelated) dilution, the fields ϵ_i become random variables with standard deviation $W \sim (d_s d_a/a_0^3)\sqrt{\nu(1 - \nu)}$, where a_0 is the lattice spacing [42]. We expect the weak correlations of the random fields to leave the previous numerical phase diagrams in $d = 1$ qualitatively unchanged [Fig. 2(d)].

This dipolar spin model becomes particularly intriguing as one varies the dimensionality of the system since the "extended-pairs" criterion predicts $d_c = 3/2$ for $\alpha = \beta = 3$. Compared to the simple Anderson criterion, which predicts $d_c = 3$, this already allows one to investigate the validity of the resonant pair counting arguments for optical lattice pancakes where $d = 2$.

An additional feature of such systems is the ability to tune the spin-flip power law. The large rotational constant B enables restriction to the Hilbert space spanned by $|\downarrow\rangle = |J = 1, m_j = -1\rangle$ and $|\uparrow\rangle = |J = 1, m_j = 1\rangle$. In this case, the dipolar flip-flop process is effectively eliminated at first order; the system instead hops two units of J^z via a second-order process of the form [see Fig. 3(e)] $H' = \sum t_{ij}^2/r_{ij}^6[(d_+^i)^2(d_-^j)^2 + (d_-^i)^2(d_+^j)^2]$, while the interaction remains formally unchanged. With the effective hopping power law increased to $\alpha = 6$ and the interaction remaining as $\beta = 3$, one finds that (in $d = 2$) all criteria for the consistency of localization are now satisfied, including both the extended-pairs criterion, which predicts $d_c \approx 2.3$, and the iterated-pairs criterion with $d_c = 2.5$.

Finally, solid-state implementations can be considered using spin defects in semiconductors. For example, nitrogen-vacancy (NV) defects in diamond [35–38] are spin-1 magnetic impurities described by the Hamiltonian

$H_{NV} = D_0 S_z^2 + \mu_e B S_z$, where D_0 is a large crystal field splitting. In the presence of an applied magnetic field, one can restrict the NV dynamics to a two-level subspace and recover the Hamiltonian of Eq. (1).

Experimental feasibility.—There are several probes available for detecting many-body localization in quantum optical systems: (1) observing arrested decay of a long-wavelength spin-number modulation, (2) generalized single-site spin-echo protocols that exhibit anomalously slow dephasing [14,15,17–19], and (3) direct measurements of real-space correlation functions. The simplest approach is to directly observe a lack of diffusion. In a typical ergodic system, an initial long-wavelength inhomogeneous spin polarization decays as $\sim e^{-Dk^2t}$, where D is the diffusion constant. For a many-body localized phase, $D = 0$. In any experiment, coupling to an external bath is unavoidable and produces characteristic decoherence time scales; T_1-type depolarization provides a uniform k-independent contribution to the overall decay. In the presence of weak Markovian T_2 dephasing, *extrinsic* energy fluctuations induce diffusion, with $D_{T_2} \sim a_0^2/T_2$ (neglecting backaction onto the bath). Since $T_2 \leq T_1$, the figure of merit in such experiments is a separation of scale between D_{T_2} and the expected ergodic diffusion, $D_e \sim a_0^2/T_{a_0}$, where T_{a_0} represents the lattice scale hopping time. Alternatively, one can also measure the decay of an initially polarized region; for a Gaussian spot of initial size ℓ (larger than any correlation length), the modulation at the origin decays as $\sim (\ell^2 + Dt)^{-d/2}e^{-t/T_1}$. Here, one hopes to extract the subexponential diffusive behavior, which can, in principle, be achieved by varying the spot size.

In the molecular case, the most direct experimental realization of our proposals would be in diatomic alkali systems [34,47–51]. Both the orbital and rotational cases can be carried out with currently available technology; indeed, the loading of $^{40}K^{87}Rb$ molecules into 1D [33] and 3D [47] lattices, as well as dipolar spin exchange [46], has already been demonstrated. For a typical polar molecule with saturated dipole moment ~ 3 Debye, the interaction strength at 532 nm (optical lattice spacing) corresponds to approximately 100 kHz, yielding $T_{a_0} \approx 10~\mu s$. Meanwhile, dephasing times of up to $T_2 \sim 100$ ms [46] and ground-state lifetimes of up to $T_1 \sim 25$ s have been observed [47].

In the case of NVs, recent advances in implantation and annealing have enabled dense defect ensembles with average spacing ~ 2–3 nm [52]. The magnetic dipolar interaction at such distances is given by $T_{a_0} \sim 1~\mu s$, significantly smaller than the typical room-temperature coherence times T_1, $T_2 \sim 10$ ms of isolated NVs (working at cryogenic temperatures can lead to further improvements [53]). To observe many-body localization in such a system will require the ability to reduce the effective dimensionality; this can be achieved by fabricating quasi-1D diamond nanopillars [54] or by controlled implantation in 2D layers [55,56].

In summary, by constructing hierarchical spin resonances, we have analyzed upper critical dimensions for many-body localization in the presence of power laws (Table I). Our

arguments suggest that MBL is accessible to AMO-type experiments involving dipolar spins in two dimensions or hopping polar molecules in three or fewer dimensions. Our work opens a number of intriguing directions: (1) generalizations to other dipolar platforms such as Rydberg atoms, trapped ions, and other spin qubits and (2) working near the upper critical dimensions to probe the nature of the MBL transition.

[1] P. W. Anderson, Phys. Rev. **109**, 1492 (1958).
[2] L. Fleishman and P. W. Anderson, Phys. Rev. B **21**, 2366 (1980).
[3] B. L. Altshuler, Y. Gefen, A. Kamenev, and L. S. Levitov, Phys. Rev. Lett. **78**, 2803 (1997).
[4] D. Basko, I. Aleiner, and B. Altshuler, Ann. Phys. (Amsterdam) **321**, 1126 (2006).
[5] I. V. Gornyi, A. D. Mirlin, and D. G. Polyakov, Phys. Rev. Lett. **95**, 206603 (2005).
[6] A. L. Burin and Y. Kagan, Zh. Eksp. Teor. Fiz. **106**, 633 (1994) [JETP **79**, 347 (1994)].
[7] A. L. Burin, Y. Kagan, L. A. Maksimov, and I. Y. Polishchuk, Phys. Rev. Lett. **80**, 2945 (1998).
[8] A. L. Burin, D. Natelson, D. D. Osheroff, and Y. Kagan, *Tunneling Systems in Amorphous and Crystalline Solids*, edited by P. Esquinazi (Springer Verlag, Berlin, 1998), pp. 223–316.
[9] A. L. Burin, arXiv:cond-mat/0611387.
[10] V. Oganesyan and D. A. Huse, Phys. Rev. B **75**, 155111 (2007).
[11] A. Pal and D. A. Huse, Phys. Rev. B **82**, 174411 (2010).
[12] M. Znidaric, T. Prosen, and P. Prelovsek, Phys. Rev. B **77**, 064426 (2008).
[13] C. Monthus and T. Garel, Phys. Rev. B **81**, 134202 (2010).
[14] J. H. Bardarson, F. Pollmann, and J. E. Moore, Phys. Rev. Lett. **109**, 017202 (2012).
[15] R. Vosk and E. Altman, Phys. Rev. Lett. **110**, 067204 (2013).
[16] S. Iyer, V. Oganesyan, G. Refael, and D. A. Huse, Phys. Rev. B **87**, 134202 (2013).
[17] M. Serbyn, Z. Papic, and D. A. Abanin, Phys. Rev. Lett. **110**, 260601 (2013).
[18] D. A. Huse and V. Oganesyan, arXiv:1305.4915.
[19] M. Serbyn, Z. Papic, and D. A. Abanin, Phys. Rev. Lett. **111**, 127201 (2013).
[20] D. A. Huse, R. Nandkishore, V. Oganesyan, A. Pal, and S. L. Sondhi, Phys. Rev. B **88**, 014206 (2013).
[21] D. Pekker, G. Refael, E. Altman, and E. Demler, Phys. Rev. X **4**, 011052 (2014).
[22] R. Vosk and E. Altman, Phys. Rev. Lett. **112**, 217204 (2014).
[23] Y. Bahri, R. Vosk, E. Altman, and A. Vishwanath, arXiv:1307.4092.
[24] B. Bauer and C. Nayak, J. Stat. Mech. (2013) P09005.
[25] B. Swingle, arXiv:1307.0507.
[26] A. Chandran, V. Khemani, C. R. Laumann, and S. L. Sondhi, Phys. Rev. B **89**, 144201 (2014).
[27] M. Schiulaz and M. Müller, AIP Conf. Proc. **1610**, 11 (2014).
[28] M. Schiulaz, A. Silva, M. Müller, arXiv:1410.4690.
[29] N. Y. Yao, C. R. Laumann, J. I. Cirac, M. D. Lukin, J. E. Moore, arXiv:1410.7407.
[30] S Korenblit *et al.*, New J. Phys. **14**, 095024 (2012).
[31] I. I. Ryabtsev, D. B. Tretyakov, I. I. Beterov, and V. M. Entin, Phys. Rev. Lett. **104**, 073003 (2010).
[32] J. Nipper, J. B. Balewski, A. T. Krupp, B. Butscher, R. Low, and T. Pfau, Phys. Rev. Lett. **108**, 113001 (2012).
[33] M. H. G. de Miranda, A. Chotia, B. Neyenhuis, D. Wang, G. Quéméner, S. Ospelkaus, J. L. Bohn, J. Ye, and D. S. Jin, Nat. Phys. **7**, 502 (2011).
[34] K. K. Ni, S. Ospelkaus, M. H. G. de Miranda, A. Peer, B. Neyenhuis, J. J. Zirbel, S. Kotochigova, P. S. Julienne, D. S. Jin, and J. Ye, Science **322**, 231 (2008).
[35] P. Neumann *et al.*, Nat. Phys. **6**, 249 (2010).
[36] L. Childress, M. V. G. Dutt, J. M. Taylor, A. S. Zibrov, F. Jelezko, J. Wrachtrup, P. R. Hemmer, and M. D. Lukin, Science **314**, 281 (2006).
[37] M. V. G. Dutt, L. Childress, L. Jiang, E. Togan, J. Maze, F. Jelezko, A. S. Zibrov, P. R. Hemmer, and M. D. Lukin, Science **316**, 1312 (2007).
[38] P. Neumann, N. Mizuochi, F. Rempp, P. Hemmer, H. Watanabe, S. Yamasaki, V. Jacques, T. Gaebel, F. Jelezko, and J. Wrachtrup, Science **320**, 1326 (2008).
[39] t_{ij}, V_{ij} do not scale with distance.
[40] L. S. Levitov, Phys. Rev. Lett. **64**, 547 (1990).
[41] L. S. Levitov, Ann. Phys. (N.Y.) **8**, 697 (1999).
[42] See Supplemental Material at http://link.aps.org/supplemental/10.1103/PhysRevLett.113.243002 for algebraic details and derivations.
[43] A. L. Burin and I. Ya. Polishchuk, arXiv:0707.2596.
[44] M. White, M. Pasienski, D. McKay, S. Q. Zhou, D. Ceperley, and B. DeMarco, Phys. Rev. Lett. **102**, 055301 (2009).
[45] J. M. Brown and A. Carrington, *Rotational Spectroscopy of Diatomic Molecules* (Cambridge University Press, Cambridge, England, 2003).
[46] B. Yan, S. A. Moses, B. Gadway, J. P. Covey, K. R. A. Hazzard, A. M. Rey, D. S. Jin, and J. Ye, Nature (London) **501**, 521 (2013).
[47] A. Chotia, B. Neyenhuis, S. A. Moses, B. Yan, J. P. Covey, M. Foss-Feig, A. M. Rey, D. S. Jin, and J. Ye, Phys. Rev. Lett. **108**, 080405 (2012).
[48] K. Aikawa, D. Akamatsu, M. Hayashi, K. Oasa, J. Kobayashi, P. Naidon, T. Kishimoto, M. Ueda, and S. Inouye, Phys. Rev. Lett. **105**, 203001 (2010).
[49] J. Deiglmayr, A. Grochola, M. Repp, K. Mörtlbauer, C. Glück, J. Lange, O. Dulieu, R. Wester, and M. Weidemüller, Phys. Rev. Lett. **101**, 133004 (2008).
[50] A. Kerman, J. Sage, S. Sainis, T. Bergeman, and D. DeMille, Phys. Rev. Lett. **92**, 033004 (2004).
[51] T. Takekoshi *et al.*, Phys. Rev. A **85**, 032506 (2012).
[52] P. C. Maurer and G. Kucsko *et al.* (to be published).
[53] N. Bar-Gill, L. M. Pham, A. Jarmola, D. Budker, and R. L. Walsworth, Nat. Commun. **4**, 1743 (2013).
[54] T. M. Babinec, B. J. M. Hausmann, M. Khan, Y. Zhang, J. R. Maze, P. R. Hemmer, and M. Lončar, Nat. Nanotechnol. **5**, 195 (2010).
[55] P. Spinicelli *et al.*, New J. Phys. **13**, 025014 (2011).
[56] D. M. Toyli, C. D. Weis, G. D. Fuchs, T. Schenkel, and D. D. Awschalom, Nano Lett. **10**, 3168 (2010).